

# Evaluating the Spatio-Temporal Distribution of Nitrogen Dioxide, Land Surface Temperature and NDVI in Nairobi City County

Patricia Mwangi

Dept. of Spatial & Environmental Planning, Kenyatta University, Nairobi, Kenya- mwangi.patricia@ku.ac.ke

**Keywords:** Air Pollution, Sentinel-5P, Nitrogen Dioxide, Land Surface Temperature, Population Density, NDVI

## Abstract

Cities are becoming larger and it is estimated that by the year 2050, more than 6 billion people will be living in cities. As cities expand and grow, the quality of life and conditions will also transform. An integral part of environmental studies has been statistical analysis in modelling the spatial dynamics of land use changes. The research involved the use of satellite imagery to determine yearly averaged values of LST and NDVI from Landsat 8 OLI/TIR and monthly mean values of Nitrogen Dioxide (NO<sub>2</sub>) from Sentinel 5-Precursor (Sentinel-5P) across Nairobi City County. The datasets covered the period 2019, 2020, 2021, 2022 and 2023 and were analysed in Google Earth Engine. Results indicated that the yearly mean values in NO<sub>2</sub> and LST in 2020 reduced by 2% and 12% respectively from 2019, while the mean NDVI value significantly increased by 28% in 2020 from 2019. NO<sub>2</sub> has a negative correlation with LST in all years and a positive correlation with NDVI. Pearson correlation with population densities in constituencies in Nairobi in 2019 and 2023 indicate a negative correlation with NDVI and a positive correlation with NO<sub>2</sub> and LST. Constituencies that have higher population densities tend to have lower vegetation densities and higher NO<sub>2</sub> concentrations and temperature. Vegetation therefore plays a crucial role in air quality and that climatic factors such as precipitation and temperature influence the concentration of pollutants.

## 1. Introduction

Air quality is considered one of the main environmental factors that directly impacts human health (Morozova et al. 2022). In 2019 the World Health Organization (WHO) estimated that 89% of the 4.2 million premature deaths that occurred annually occurred in middle-to-low income countries. These countries disproportionately experience the burden of air pollution with respiratory and cardiovascular diseases occurring due to exposure to fine particles (WHO 2022). Harmful effects of air pollution affect all age groups, with children, women and elderly being the most vulnerable (Hassaan et al. 2023). Air pollution also significantly causes damage to crops and buildings.

The UN has estimated that the urban population will reach more than 6 billion people by the year 2050 (Marans 2012). Formation of urban heat island (UHI) can be linked to increased densities in population and built-up areas, reduced vegetation cover, increased trapping and absorption of incoming solar radiation in built-up areas (Lee et al. 2020). Urbanization contributes to changing climatic conditions (Mwangi et al. 2020) and is one of the factors in the creation of UHI (Matsaba et al. 2020).

LST is an important phenomenon due to its relationship with different biophysical factor in the environment as it is affected by the amount of vegetation cover in an area, built-up materials. There have been positive links between LST and several pollutant gases in urban areas such as nitrogen dioxide (NO<sub>2</sub>), carbon monoxide (CO) and Ozone (O<sub>3</sub>) (Rahaman et al. 2023). Urban sprawl encourages the use of motorized modes of transport hence increases emissions. Nyaga (2014) determined a relationship between land surface temperature and air quality, with areas in fringes of Nairobi having lower correlations compared to areas within the CBD. Concentrations of particulate matter was lower in fringe areas than built-up areas.

A major contributor to outdoor air pollution is the road transportation sector as it primarily relies on fossil fuel combustion thus making it the largest source of regional and urban air pollution (Wang et al. 2019; Li and Managi 2021). In 2010, it accounted for 61% of the total nitrous oxide emissions, 39% of fine particulate matter and 20% of carbon in Kenya (Mbandi et al. 2023).

## 1.2 Sentinel -5 Precursor

Sentinel-5 Precursor (Sentinel-5P), the first mission by Copernicus to monitor the atmosphere, was launched on 13<sup>th</sup> October 2017. To monitor aerosols and trace gases critical in determining air quality and climate, the satellite carries the Tropospheric Monitoring Instrument (TROPOMI) (ESA 2024), by measuring the magnitude of reflected sunlight by the atmosphere in the visible, near and mid-infra-red region (Rahaman et al. 2023). The satellite delivers high-resolution images of pollutants in the atmosphere such as ozone, nitrogen dioxide, carbon monoxide, formaldehyde, sulphur dioxide, methane and aerosols (eoPortal 2012; Hassaan et al. 2023).

In Google Earth Engine (GEE), Sentinel-5P Offline catalog (OFFL) Nitrogen Dioxide is available at a spatial resolution of 1113.2 meters (Google for Developers 2024a). Nitrogen Dioxide is one of the six widespread air pollutants whose limits in the outdoor air have been set through national air standards. The main contributors of NO<sub>2</sub> in metropolitan areas come from domestic heating, electricity generation, traffic and ozone/ NO<sub>x</sub> equilibrium. Nitrogen dioxide (NO<sub>2</sub>) is an important pollutant studied in urban areas as it's released into the lower atmosphere through processes such as combustion, burning of fossil fuels, while in the upper atmospheres it occurs through lightening (Rahaman et al. 2023). Satellite imagery has been extensively used to determine air quality over cities, and integrated with ground monitoring stations. Angom et al, (2019) compared

satellite measurements of NO<sub>2</sub> from Aura satellite imagery with absorbing aerosol index (AAI) data from Tropospheric Emission Monitoring Internet Service.

Therefore, data from Sentinel-5P provides information on atmospheric pollution and can be used to determine air quality and emission hotspots (Tonion and Pirotti 2022). This study seeks to determine the influence of changes in land surface temperature, vegetation health and population density on nitrogen dioxide (NO<sub>2</sub>) across the constituencies in Nairobi City.

## 2. Methodology

### 2.1 Study Area

Nairobi is the capital of Kenya and the largest city in East and Central of Africa. It is centrally located geographically at 1°9' S, 1°28' S and 36°4' E, 37°10' E, with an area of 684 Km<sup>2</sup>. Nairobi City County (NCC) has two rainy seasons with long rains from March-May (MAM), with its peak in April and the short rains from October-December (OND) with its peak in November. The lowest temperatures are normally recorded in June-August (JJA) while the highest temperatures are in December to March (Ongoma et al. 2018).

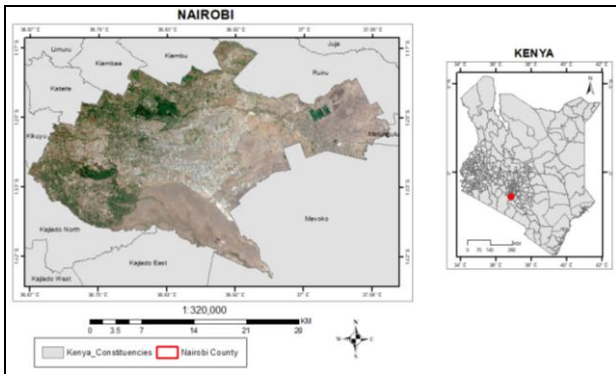


Figure 1 : Location Map of Nairobi City County

### 2.2 Processing Landsat 8 OLI/TIR Satellite Imagery

The Google Earth Engine (GEE) tool was used to process satellite imagery for the period 2019, 2020, 2021, 2022 and 2023. USGS Landsat 8 OLI/TIRS Collection 2, Tier 1-Level 2, atmospheric surface reflectance datasets were imported into GEE and a scaling factor (USGS 2024;Google for Developers 2024; Ridho 2023) applied to all optical bands (equation 1) and thermal bands (equation 2) .

$$SB_x = SR_{B_x} * 0.0000275 + (-0.2) \quad (1)$$

Where:

$x$  optical band  
 $SB_x$  scaled optical band  
 $SR_{B_x}$  Surface reflected band

$$TB_t = ST_{B_t} * 0.00341802 + (149.0) \quad (2)$$

Where:

$t$  thermal band 10 or 11  
 $TB_t$  scaled thermal band  
 $ST_{B_t}$  surface reflectance thermal band

A function was applied to mask clouds and cloud shadows in Landsat 8 Imagery by defining the cloud shadow and cloud

bitmasks as Bits 3 and 5. Elimination of cloud and cloud shadows was done by creating a binary mask to identify clear conditions.

### 2.3 Normalized Difference Vegetation Index

Zha et al. (2003) developed normalized difference built-up index (NDBI) to analyse and identify built-up areas. As-syakur et al. (2012) compared five indices, NDBI, Urban Index (UI), EBBI, IBI and NDBaI in mapping built-up areas to map the distribution of vegetation and a variety of conditions over land surfaces normalized difference vegetation index (NDVI). Zhou et al., (2021) used NDVI to determine the correlation and spatial characteristic of air pollution across China during COVID-19 lockdown. Therefore NDVI was used to map the healthy vegetation and also determine the role it plays in air quality (equation 3).

$$NDVI = \frac{Band5 - Band4}{Band5 + Band4} \quad (3)$$

### 2.4 Land Surface Temperature Computation

**2.4.1 Vegetation portion:** The vegetation portion was calculated as:

$$V_p = \left( \frac{NDVI - NDVI_{min}}{NDVI_{max} - NDVI_{min}} \right)^2 \quad (4)$$

Where:

$V_p$  Vegetation portion  
 $NDVI$  Normalized difference vegetation index  
 $NDVI_{min}$  Minimum NDVI  
 $NDVI_{max}$  Maximum NDVI

Land surface emissivity (LSE) was computed as (Ermida et al. 2020) (Equation 5):

$$LSE = 0.004 * V_p + 0.986 \quad (5)$$

**2.4.2 Land Surface Temperature:** The land surface emissivity and at-satellite brightness were used to calculate the land surface temperature in Celsius (Equation 6):

$$LST = \left[ \frac{T_{SB}}{(1 + (\lambda \cdot \frac{T_{SB}}{\rho}) \cdot \ln(LSE))} \right] - 273.15 \quad (6)$$

Where:

$LST$  Land surface temperature  
 $T_{SB}$  At-satellite brightness temperature  
 $\lambda$  Wavelength of emitted radiance ( $\lambda = 11.5\mu m$ )  
 $\rho$   $h * \frac{c}{\sigma} (1.438 * 10^{-2} m K)$   
 $\sigma$  Boltzmann's constant ( $1.38 * 10^{-23} J K^{-1}$ )  
 $h$  Planck's constant ( $6.26 * 10^{-34} J s$ )  
 $c$  Velocity of light ( $2.998 * 10^8 m s^{-1}$ )

### 2.5 Processing Sentinel-5P Satellite Imagery

Air quality data was processed from Sentinel-5P TROPOMI NRTI L3 NO<sub>2</sub> (NO<sub>2</sub>\_column\_number\_density in the unit of mol/m<sup>2</sup>) dataset. Mean values for each month and year were processed and downloaded. Administrative boundaries over Nairobi were then used to extract data across the city to determine the spatio-temporal variation of NO<sub>2</sub>, LST and NDVI

across the city. These datasets were then exported and analysed in ArcMap 10.8.2 and statistical analysis carried out in STATA.

## 2.6 Precipitation Data

Mean monthly precipitation data from 2019 to 2023 was freely downloaded from Africa Data Hub (2023) and it is from GloH2O and has been modelled at a global scale.

<https://www.africadatahub.org/data-resources/climate-observer?city=nairobi>

## 3. Results

### 3.1 Nitrogen Dioxide Concentrations

Average monthly NO<sub>2</sub> values (mol/m<sup>2</sup>) for each year from 2019 to 2023 are shown in Figure 2. Restriction of movement into and out of the Nairobi Metropolitan area due to COVID-19 pandemic commenced on April 2020 with persons continuing with their activities within the specified jurisdictions (RoK 2020). These restrictions were partially lifted in June 2020, with curfew times still in place. Minimal movement and activities resulted in a mean reduction in NO<sub>2</sub> and LST in 2020 (Table 1). The NO<sub>2</sub> values started increasing after April 2021, with a peak in November 2021.

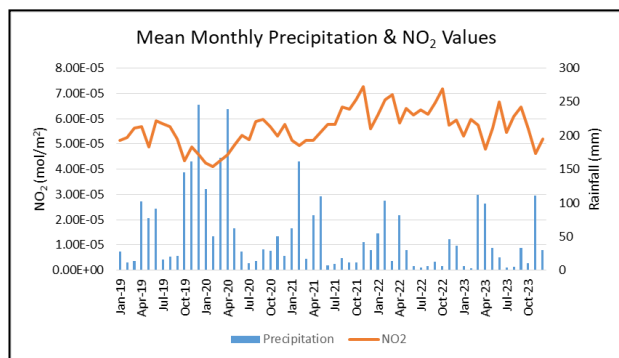


Figure 2: Mean monthly values of precipitation and NO<sub>2</sub> from 2019 to 2023

Low concentrations in each year were recorded in the months of October (2019), February (2021 & 2022) and November (2022 & 2023). Higher concentrations were recorded in the months of June (2019), September (2020), November (2021), October (2022) and June (2023). There was a decline in NO<sub>2</sub> concentrations from October 2019 to February 2020 which could be attributed to the short rains that started in early October 2019 and lasted till January 2020. These rains, recorded as one of the wettest since 1985 in East Africa, were attributed to a strong positive Indian Ocean Dipole (IOD) occurrence in the Indian Ocean. In late October 2021 all COVID-19 restrictions were lifted which could indicate an increase in NO<sub>2</sub> concentrations especially in November 2021. Other climatic factors such as wind patterns and temperature influence the concentration of pollutants. In 2022, in the months of October-December (OND), the distribution of rainfall recorded was poor in space and time throughout Kenya, with temperatures in this year reported to be higher than average (RoK 2022) and hence could have impacted NO<sub>2</sub> values in October 2022. However, low concentration in 2022 and 2023 were during the short rains while high values in June were in the dry period.

Rahaman et al. (2023) determined that between 2019 and 2021, during COVID-19 lockdown, NO<sub>2</sub> concentrations were higher

during winter and lower in the summer period. Kalisa et al. (2022) study of air pollution across East Africa determined high pollution periods in the months of February-March and June-July, while low pollution periods between the period of April-May and October- November. Oguge et al. (2024) analysis of PM<sub>2.5</sub> in Nairobi using in-situ monitoring stations determined seasonal fluctuations in concentrations particularly in the wet seasons of April and were highest in the dry-cold periods of July and August. This may be due to weather conditions as this is during the rainy seasons.

### 3.2 Correlation between NO<sub>2</sub>, LST and NDVI

The lowest mean values in NO<sub>2</sub> and LST are recorded in 2020 which is a 2% and 12% reduction respectively from 2019. The mean NDVI value significantly increased by 28% in 2020 from 2019 indicating the likely impact of restricted human movement on the health of vegetation. In 2023 the mean NO<sub>2</sub> values increased by 7% while the mean temperature decreased by 6% from 2019 mean values. Rahaman et al. (2023) analysed the relationship between NO<sub>2</sub>, LST and vegetation indices from satellite imagery during winter and summer seasons.

Year	NO <sub>2</sub> (mol/m <sup>2</sup> )	LST (°C)	NDVI
2019	5.25E-05	38.31	0.40
2020	5.11E-05	33.77	0.51
2021	5.82E-05	35.48	0.43
2022	6.36E-05	36.61	0.41
2023	5.63E-05	35.93	0.43

Table 1: Mean values across the years

Angom et al, (2019) used Aura satellite imagery to determine changes in NO<sub>2</sub> concentrations before and after the pandemic in Dar es Salaam, Nairobi and Kampala in East Africa. Results indicated a significant reduction in emissions by 6% in Kampala and 8.91% in Nairobi, while in Dar es Salaam there was an increase in emissions since lock-down was not enforced. Almagbile and Hazaymeh (2023) study of NO<sub>2</sub> and CO using Sentinel-5P during the lockdown period in Amman city, Jordan indicated a reduction of these emissions and a reduction in LST, extracted from MODIS.

Pearson correlation analysis between LST and NDVI (Table 2) indicates a strong negative linear correlation between the two variables across all years. This implies that as vegetation health and density decreases, the LST within the same area increases. Previous studies by Odunuga et al., (2015); Zhao et al., (2018) and; Mwangi et al., (2018) showed a positive correlation with built-up areas due to the thermal capacity of impervious surfaces.

Year	2019	2020	2021	2022	2023
NDVI	-0.70	-0.74	-0.73	-0.72	-0.67

Table 2: Pearson correlation with LST

Correlation analysis of NO<sub>2</sub> and NDVI (Table 3) shows a positive correlation in all years except 2020 where there is a negative correlation. There is a negative correlation with LST in all years signifying that areas with lower surface temperatures tend to have higher concentrations of NO<sub>2</sub>. Pearson correlation results by Rahaman et al. (2023) between two cities Delhi and Dhakar determined a negative correlation between NO<sub>2</sub> and vegetation indices, but demonstrated a positive correlation with LST. This implied that NO<sub>2</sub> increased with reduced vegetation

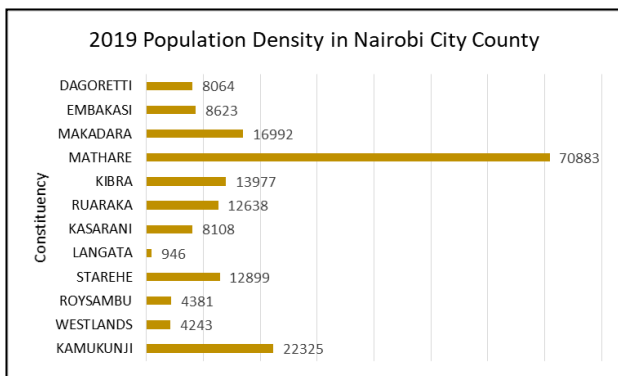
density. The differences in observations between different cities and geographical areas indicates the intrinsic dynamic temporal behaviour between environmental factors.

Year	2019	2020	2021	2022	2023
LST (°C)	-0.37	-0.01	-0.23	-0.31	-0.34
NDVI	0.12	-0.07	0.06	0.11	0.15

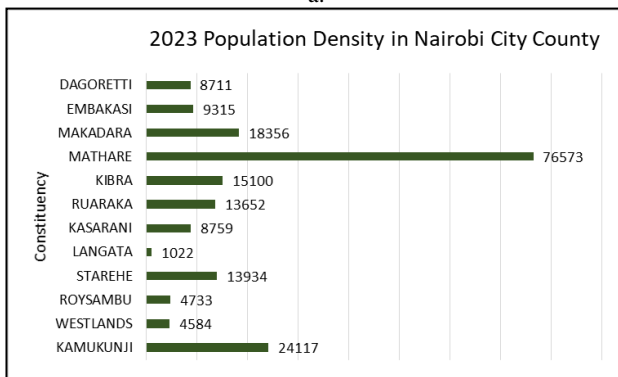
Table 3: Pearson correlation of NO<sub>2</sub> (mol/m<sup>2</sup>)

### 3.3 Spatio-Temporal Analysis in Constituencies

The spatio-temporal distribution of LST and NO<sub>2</sub> in 2019 and 2023 was evaluated across the different administrative boundaries in Nairobi and their correlation with population densities. The population census done in 2019 determined that the total population of Nairobi was 4,337,080 (RoK 2019a). The analysis was done only between 2019 and 2023 to appreciate the impact of population growth on LST, NDVI and NO<sub>2</sub> between the four year period.



a.



b.

Figure 3: Population density in 2019 (a) and 2023 (b)

Mathare constituency has the highest population density in Nairobi while Langata has the lowest population density (Figure 3). Nairobi City County has at least fifteen (15) informal settlements with Kibera slum being the second largest in Africa. Other informal settlements are spread across the city in Mathare, Kamukinjji, Kibra, Embakasi, Langata and other constituencies. Mathare informal settlement is a group of 13 villages and is the second largest after Kibera in Kenya (UN-Habitat 2020).

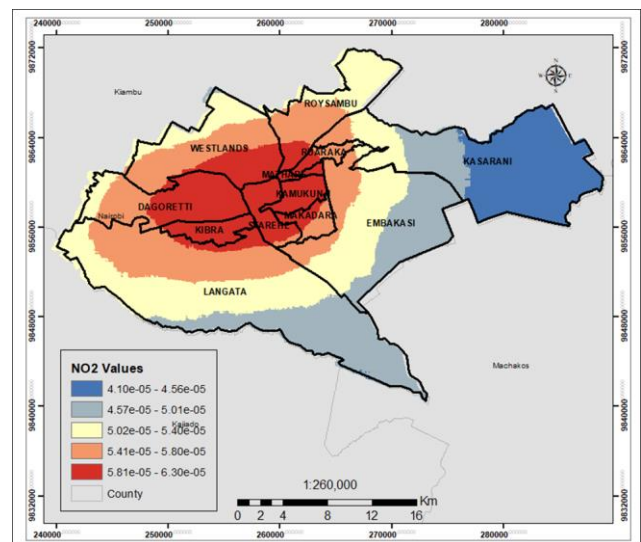
It was projected that by the year 2023, Nairobi's population would reach 4,750,056 (RoK, 2019). This is approximately 4.12% annual population increase from 2019. It is estimated that nearly 2 million people live in Nairobi's slums, and this is approximately 1% of the city's geographical area (Faye 2023).

The effect of city size or population density on air quality is important to evaluate. Results of the correlation analysis between population densities and NO<sub>2</sub>, LST and NDVI in the years 2019 and 2023 are in Table 4.

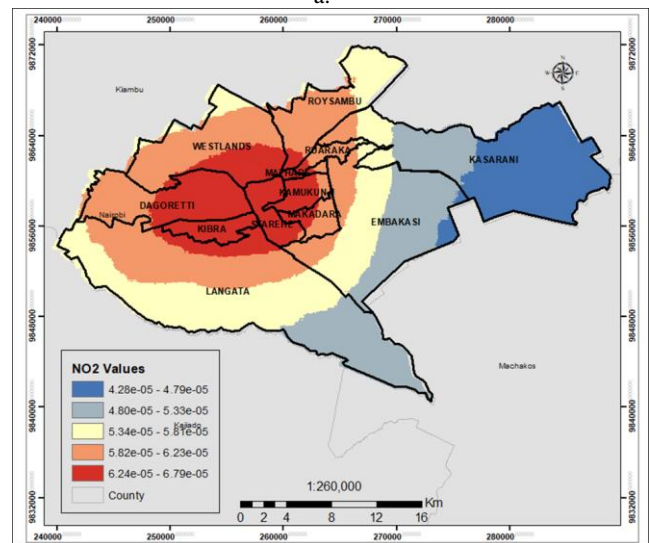
Value	NO <sub>2</sub>	LST	NDVI
2019	0.48	0.31	-0.58
2023	0.31	0.34	-0.53

Table 4: Pearson correlation with population density in Nairobi

Table 4 indicates that population density relates positively with NO<sub>2</sub> and LST in both 2019 and 2023. There is a negative correlation with NDVI which therefore implies that with increased population, vegetated areas are replaced by impervious surfaces, hence an increased built-up density. There was a reduced correlation in NO<sub>2</sub> in 2023 compared to 2019 despite an increment in population and NO<sub>2</sub> levels. Kaplan and Avdan (2020) integrated Sentinel-5P CO and NO<sub>2</sub> datasets with digital elevation model (DEM), population statistics and vegetation data and determined a positive correlation with population densities and negative correlation with elevation of both pollutants.



a.



b.

Figure 4: NO<sub>2</sub> dispersal in 2019 (a) and 2023 (b)



Figure 4 indicates a concentration of NO<sub>2</sub> in the central business district due to human activities and emissions from vehicles. Nairobi is ranked as one of the most congested cities in the world due to increased traffic snarl-ups leading to reduced commuting time (ITDP 2020). It is critical to understand the spatiotemporal distribution of LST and NO<sub>2</sub> across the constituencies as urban morphology and land cover plays a role in the dispersal of air pollutants and heat as taller buildings reduce wind speed.

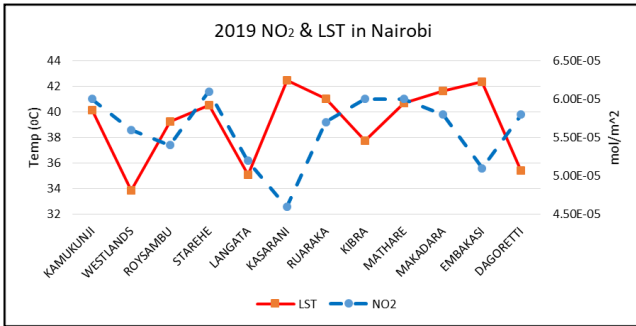


Figure 5: NO<sub>2</sub> and LST values in 2019

Mathare has the highest population density with a mean temperature of 41°C and NO<sub>2</sub> value of 6.00E-05 (Figure 5). Mean temperatures in 2019 of Westlands, Langata and Dagoretti constituencies, which have higher vegetation coverage, are between 34°C and 35°C. Kasarani and Embakasi located in the eastern parts of Nairobi have lower NO<sub>2</sub> concentrations compared to other constituencies. The main land cover in these areas is grassland with NDVI values of 0.2-0.4, which would indicate the high LST values in both 2019 and 2023. Land tends to warm-up faster than built-up areas during the day and cool faster at night than concrete, emitting absorbed thermal heat at night in long wave radiation. These differences in land cover interactions with LST constitutes to the urban heat island effect.

Nairobi's central business district is located in Starehe constituency and it has the highest emissions in both 2019 and 2023 at 6.10E-05 mol/m<sup>2</sup> and 6.60E-05 mol/m<sup>2</sup> respectively. LST in this area in 2019 and 2023 is 41°C and 37°C respectively. Kamukunji and Makadara constituency are comprised mainly of commercial and industrial activities have LST values of 40°C, 42°C respectively and NO<sub>2</sub> values of 6.00E-05 mol/m<sup>2</sup> and 5.80E-05 mol/m<sup>2</sup> respectively in 2019. Kibra and Mathare constituencies which have the largest slums in Nairobi do not have corresponding high temperatures which may be due to material type of structures in the area in respect to absorbing incoming short-wave radiation. However, emissions in this area are both at 6.00E-05 mol/m<sup>2</sup>.

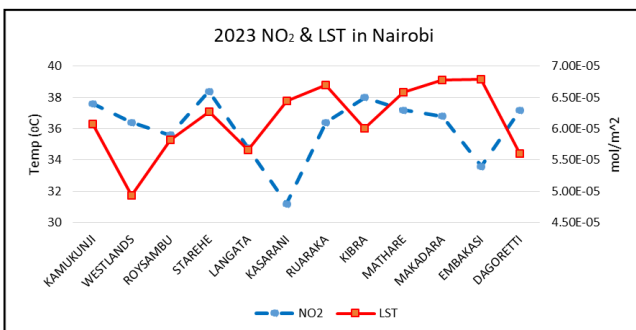
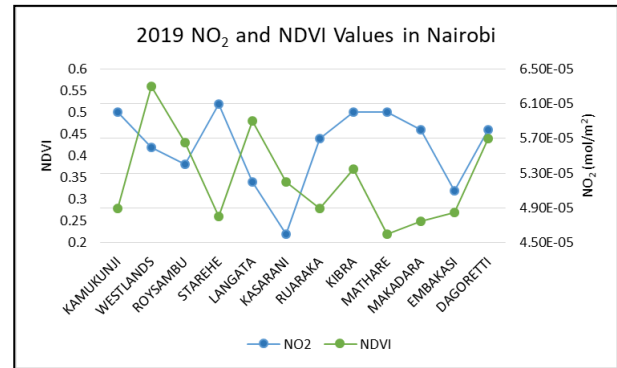
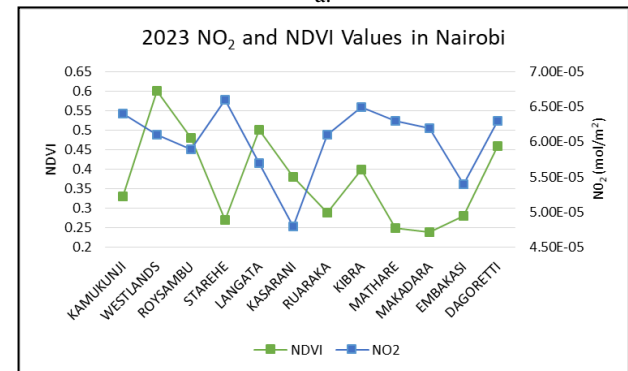


Figure 6: NO<sub>2</sub> and LST values in 2023

Figure 6 indicates a similar trend in distribution of NO<sub>2</sub> and LST concentrations in 2019. Areas that are densely populated especially due to commercial and industrial activities had corresponding high LST and NO<sub>2</sub> values. Kasarani and Embakasi have lower NO<sub>2</sub> values in both 2019 and 2023 with corresponding high temperatures. Oyugi (2021) analysis of air quality distribution in Nairobi determined that there was a decreased concentration of gases away from the Central Business District (CBD), industrial and satellite commercial areas in the city. Hassaan et al. (2023) determined that the distribution pattern of CO concentrations dependent on the distance from the main source of emission.



a.



b.

Figure 7: NDVI and NO<sub>2</sub> values in 2019 (a) and 2023 (b)

As indicated in Table 4 the negative correlation between population densities and NDVI is seen per constituency in Figure 7 where areas with higher NO<sub>2</sub> concentrations have lower NDVI values. Populated areas such as Kamukunji, Starehe, Mathare, Makadara and Embakasi have higher built-up densities therefore lower NDVI values. Constituencies with high NDVI values are Westlands, Langata and Dagoretti due to Nairobi Arboretum, Ngong, Karura, Ololua forests and are located on the north and western parts of Nairobi. The seasonal variation of NDVI with NO<sub>2</sub> within each year was not studied but the spatial variation of values across Nairobi indicates that vegetation plays a crucial role in air quality. In Delhi, Rani and Kumar (2023) observed higher pollution values when NDVI and Enhanced Vegetation Index (EVI) values were low in summer due to changes in vegetation health while lower values of gaseous pollutants were observed in areas with dense vegetation. Dai et al. (2023) study of effects of different plant communities along urban streets determined that plant structure, both height and canopy plays a crucial role in the amount of NO<sub>2</sub> concentration. Results indicated that green spaces along the road effectively reduced the amount of NO<sub>2</sub> concentration. Further canopy structure and density is a crucial factor as it can lead to an increase in NO<sub>2</sub>

concentrations if there is no air flow. This research therefore elucidates that the spatio-temporal variations in NO<sub>2</sub> concentrations are influenced by human activities, climatic changes and environmental conditions such as vegetation densities.

#### 4. Conclusion and Outlook

The paper investigated the spatio-temporal variations of population densities, LST and NDVI and how they influence NO<sub>2</sub> across the city. Study shows that urban morphological variations across the city have had an influence in the interaction between LST, NO<sub>2</sub> and NDVI. The study gives insights on the spatial distribution of built-up and vegetation densities and how this may influence the distribution of populations in a city. This can be seen by the number of people living in slums in urban areas, where social amenities may not be available. The population distribution densities indicate the impact it has on vegetation since densely populated areas have a higher percentage of impervious surfaces than greenery. Increased urban developments in form of impervious surfaces such as roads, buildings lead to heat retention during the day, and interaction with different pollutants results to development of major health issues and consequences of acid rain on building façades. The expansion of roads within Nairobi Metropolitan has brought about urban sprawl, leading to increased vehicular movement and consequently increased vehicular emissions. Urban morphology also plays a key role in the dispersal of air pollutants as tall buildings causes attenuation of wind leading to higher LST and concentration of air pollutants especially along alleys. Vegetation play as vital role in mitigating against high temperatures through shading and evapotranspiration and also reducing air pollution by absorbing harmful gases, thus preserving clean air. Studies on European tree species indicated that they were responsible for a reduction of NO<sub>2</sub> concentrations in the atmosphere (Rahaman et al. 2023). Areas that are densely populated in the central parts of the city would be suitable sites for urban re-greening strategies and engagement with the community by raising awareness on various mitigation measures. Through this study, one can determine the quality of life of the population by evaluating environmental factors and determining areas of potential health risks due to prolonged exposure to urban heat and pollutants. It would therefore enable the city and national governments to develop strategies and implement policies that would ensure the sustainable growth of cities, thus making them safe and livable.

#### 5. References

- Africa Data Hub. 2023. "Climate Observer." Climate Observer. July 28, 2023. <https://www.africadatahub.org/about-climate-observer>.
- Almagbile, Ali, and Khaled Hazaymeh. 2023. "Spatiotemporal Variability/Stability Analysis of NO<sub>2</sub>, CO, and Land Surface Temperature (LST) during COVID-19 Lockdown in Amman City, Jordan." *Geo-Spatial Information Science* 26 (3): 540–57. <https://doi.org/10.1080/10095020.2022.2066575>.
- Angom, Juliet, Christopher Angiro, and Timothy Omara. 2019. "Air Quality Improvement from COVID-19 Lockdown in the East African Community: Evidences from Kampala and Nairobi Cities." *Journal* 2021 8: 7389. <https://doi.org/10.4236/oalib.1107389>.
- As-syakur, Abd Rahman, I. Wayan Sandi Adnyana, I. Wayan Arthana, and I. Wayan Nuarsa. 2012. "Enhanced Built-UP and Bareness Index (EBBI) for Mapping Built-Up and Bare Land in an Urban Area." *Remote Sensing* 4 (10): 2957–70. <https://doi.org/10.3390/rs4102957>.
- Dai, Anqi, Congzhe Liu, Yaou Ji, Qianqian Sheng, and Zunling Zhu. 2023. "Effect of Different Plant Communities on NO<sub>2</sub> in an Urban Road Greenbelt in Nanjing, China." *Scientific Reports* 13 (1). <https://doi.org/10.1038/S41598-023-30488-0>.
- eoPortal. 2012. "Copernicus: Sentinel-5P ." EoPortal. June 14, 2012. <https://www.eoportal.org/satellite-missions/copernicus-sentinel-5p#operational-systemservice-allocations>.
- Ermida, Sofia L., Patrícia Soares, Vasco Mantas, Frank M. Götsche, and Isabel F. Trigo. 2020. "Google Earth Engine Open-Source Code for Land Surface Temperature Estimation from the Landsat Series." *Remote Sensing* 12 (9): 1–21. <https://doi.org/10.3390/RS12091471>.
- European Space Agency. 2024. "Sentinel-5P." Global Air Monitoring for Copernicus. 2024. [https://www.esa.int/Applications/Observing\\_the\\_Earth/Copernicus/Sentinel-5P](https://www.esa.int/Applications/Observing_the_Earth/Copernicus/Sentinel-5P).
- Faye, Malang. 2023. "Urban Slums and Inequality in Nairobi (Kenya): A Theoretical Perspective." *Academic Review of Humanities and Social Sciences* 6 (1): 60–82. <https://doi.org/10.54186/arthuss.1160864>.
- Google for Developers. 2024a. "Sentinel-5P OFFL NO<sub>2</sub>: Offline Nitrogen Dioxide ." Earth Engine Data Catalog . 2024. [https://developers.google.com/earth-engine/datasets/catalog/COPERNICUS\\_S5P\\_OFFL\\_L3\\_NO2](https://developers.google.com/earth-engine/datasets/catalog/COPERNICUS_S5P_OFFL_L3_NO2).
- Google for Developers. 2024b. "USGS Landsat 8 Level 2, Collection 2, Tier 1 ." Earth Engine Data Catalog . 2024. [https://developers.google.com/earth-engine/datasets/catalog/LANDSAT\\_LC08\\_C02\\_T1\\_L2](https://developers.google.com/earth-engine/datasets/catalog/LANDSAT_LC08_C02_T1_L2).
- Hassaan, Mahmoud A., Salwa M. Abdallah, El Sayed A. Shalaby, and Amir A. Ibrahim. 2023. "Assessing Vulnerability of Densely Populated Areas to Air Pollution Using Sentinel-5P Imageries: A Case Study of the Nile Delta, Egypt." *Scientific Reports* 2023 13:1 13 (1): 1–11. <https://doi.org/10.1038/s41598-023-44186-4>.
- Institute for Transportation and Development Policy. 2020. "Solutions to Nairobi's Transport Challenges ." Transport Journal. May 15, 2020. <https://africa.itdp.org/finding-real-solutions-to-nairobis-transport-challenges/>.
- Kalisa, Wilson, Jiahua Zhang, Tertsea Igbawua, Malak Henchiri, Mulinga Narcisse, Deborah Nibagwire, and Mycline Umhuza. 2022. "Spatial and Temporal Heterogeneity of Air Pollution in East Africa." *SSRN Electronic Journal*, December. <https://doi.org/10.2139/SSRN.4309487>.
- Kaplan, Gordana, and Zehra Yigit Avdan. 2020. "Space-Borne Air Pollution Observation from Sentinel-5P Tropomi: Relationship between Pollutants, Geographical and Demographic Data." *International Journal of Engineering and Geosciences (IJEG)* 5: 130–37. <https://doi.org/10.26833/ijeg.644089>.

- Lee, Kyungil, Yoonji Kim, Hyun Chan Sung, Raeik Jang, Jieun Ryu, and Seong Woo Jeon. 2020. "Trend Analysis of Urban Heat Island Intensity According to Urban Area Change in Asian Mega Cities." *Sustainability*, 11.
- Li, Chao, and Shunsuke Managi. 2021. "Contribution of On-Road Transportation to PM<sub>2.5</sub>." *Scientific Reports 2021 11:1* 11 (1): 1–12. <https://doi.org/10.1038/s41598-021-00862-x>.
- Marans, Robert W. 2012. "Quality of Urban Life Studies: An Overview and Implications for Environment-Behaviour Research." *Procedia - Social and Behavioral Sciences* 35 (December 2011): 9–22. <https://doi.org/10.1016/j.sbspro.2012.02.058>.
- Matsaba, Emmanuel Ochola, Ines Langer, Aggrey Ochieng Adimo, John Bosco Mukundi, John Mwibanda Wesonga, Emmanuel Ochola Matsaba, Ines Langer, Aggrey Ochieng Adimo, John Bosco Mukundi, and John Mwibanda Wesonga. 2020. "Spatio-Temporal Variability of Simulated 2 m Air Temperature for Nairobi City, Kenya." *Current Urban Studies* 8 (2): 205–21. <https://doi.org/10.4236/CUS.2020.82011>.
- Mbandi, Aderiana Mutheu, Christopher S. Malley, Dietrich Schwela, Harry Vallack, Lisa Emberson, and Mike R. Ashmore. 2023. "Assessment of the Impact of Road Transport Policies on Air Pollution and Greenhouse Gas Emissions in Kenya." *Energy Strategy Reviews* 49 (September): 101120. <https://doi.org/10.1016/j.esr.2023.101120>.
- Morozova, A. E., O. S. Sizov, P. O. Elagin, N. A. Agzamov, A. V. Fedash, and N. E. Lobzhanidze. 2022. "Integral Assessment of Atmospheric Air Quality in the Largest Cities of Russia Based on TROPOMI (Sentinel-5P) Data for 2019–2020." *Cosmic Research* 60 (4): S57–68. <https://doi.org/10.1134/S0010952522700071>.
- Mwangi, P. W., F. N. Karanja, P. K. Kamau, and S. C. Letema. 2020. "Impact of Urban Forms on 3D Built-up Intensity Expansion Rate from Aerial Stereo-Imagery." *ISPRS Annals of the Photogrammetry, Remote Sensing and Spatial Information Sciences* V-4–2020: 6. <https://doi.org/10.5194/isprs-annals-V-4-2020-203-2020>.
- Mwangi, Patricia, Faith Karanja, and Peter Kamau. 2018. "Analysis of the Relationship between Land Surface Temperature and Vegetation and Built-Up Indices in Upper-Hill, Nairobi." *Journal of Geoscience and Environment Protection* 06 (01): 1–16. <https://doi.org/10.4236/gep.2018.61001>.
- Nyaga, Eva. 2014. "Air Quality as a Factor of Urban Heat Islands Phenomena: A Case Study of Nairobi." *Environment and Urbanization* 1 (1): 1–9. <https://doi.org/10.1007/s13398-014-0173-7.2>.
- Ogunuga, Shakirudeen, and Gbolahan Badru. 2015. "Landcover Change, Land Surface Temperature, Surface Albedo and Topography in the Plateau Region of North-Central Nigeria." *Land* 4 (2): 300–324. <https://doi.org/10.3390/land4020300>.
- Oguge, Otienoh, Joshua Nyamondo, Noah Adera, Lydia Okolla, Beldine Okoth, Stephen Anyango, Augustine Afulo, Abera Kumie, Jonathan Samet, and Kiros Berhane. 2024. "Fine Particulate Matter Air Pollution and Health Implications for Nairobi, Kenya." *Environmental Epidemiology* 8 (3): E307. <https://doi.org/10.1097/EE9.0000000000000307>.
- Ongoma, Victor, Haishan Chen, Chujie Gao, and Phillip Obaigwa Sagero. 2018. "Variability of Temperature Properties over Kenya Based on Observed and Reanalyzed Datasets." *Theoretical and Applied Climatology* 133 (3–4): 1175–90. <https://doi.org/10.1007/S00704-017-2246-Y>.
- Oyugi, Maurice O. 2021. "Urbanisation Footprints and the Distribution of Air Quality in Nairobi City, Kenya." *Journal of Environmental and Earth Sciences* 3 (2): 14–44. <https://doi.org/10.30564/jees.v3i2.3289>.
- Rahaman, Sk Nafiz, S. M. Masum Ahmed, Mohammad Zeyad, and Abid Hasan Zim. 2023. "Effect of Vegetation and Land Surface Temperature on NO<sub>2</sub> Concentration: A Google Earth Engine-Based Remote Sensing Approach." *Urban Climate* 47 (December 2022): 101336. <https://doi.org/10.1016/j.uclim.2022.101336>.
- Rani, Archana, and Manoj Kumar. 2023. "Seasonal Changes in Air Pollutants and Their Relation to Vegetation over the Megacity Delhi National Capital Region." In *Environmental Sciences Proceedings*, 27:16. Multidisciplinary Digital Publishing Institute. <https://doi.org/10.3390/ECAS2023-15119>.
- Republic of Kenya. 2019a. *2019 Kenya Population and Housing Census- Volume 1: Population by County and Sub-County. 2019 Kenya Population and Housing Census*. Vol. I. <https://www.knbs.or.ke/?wpdmpromo=2019-kenya-population-and-housing-census-volume-i-population-by-county-and-sub-county>.
- Republic of Kenya. 2019b. "Summary Report on Kenya's Population Projections." Vol. 2019.
- Republic of Kenya. 2020. *The Public Health Act. Kenya Gazette Supplement No.77*. Republic of Kenya.
- Republic of Kenya. 2022. "Climate Outlook for January 2023, Review for December 2022 and Seasonal Performance of October-December 2022 'Short-Rains.'" Nairobi. <http://www.meteo.go.ke>.
- Ridho, Muhammad. 2023. "Analyzing Land Surface Temperature (LST) with Landsat 8 Data in Google Earth Engine ." Medium. September 2023. <https://medium.com/@ridhomuh002/analyzing-land-surface-temperature-lst-with-landsat-8-data-in-google-earth-engine-f4dd7ca28e70>.
- Tonion, F., and F. Pirotti. 2022. "Sentinel-5P No<sub>2</sub> Data: Cross-Validation and Comparison With Ground Measurements." *International Archives of the Photogrammetry, Remote Sensing and Spatial Information Sciences - ISPRS Archives* 43 (B3-2022): 749–56. <https://doi.org/10.5194/isprs-archives-XLIII-B3-2022-749-2022>.
- UN-Habitat. 2020. "Informal Settlements' Vulnerability Mapping in Kenya. Facilities and Partners Mapping in Nairobi and Kisumu Settlements: The Case of Mathare."
- USGS. 2024. "Landsat Collection 2 Level-2 Science Products ." Landsat Missions. 2024. <https://www.usgs.gov/landsat>

missions/landsat-collection-2-level-2-science-products.

Wang, Ting, John Harvey, Alissa Kendall, Susan C Anenberg, Joshua Miller, Daven K Henze, Ray Minjares, and Pattanun Achakulwisut. 2019. "The Global Burden of Transportation Tailpipe Emissions on Air Pollution-Related Mortality in 2010 and 2015." *Environmental Research Letters* 14 (September). <https://doi.org/10.1088/1748-9326/ab35fc>.

World Health Organization. 2022. "Ambient (Outdoor) Air Pollution." World Health Organization. December 19, 2022. [https://www.who.int/news-room/fact-sheets/detail/ambient-\(outdoor\)-air-quality-and-health](https://www.who.int/news-room/fact-sheets/detail/ambient-(outdoor)-air-quality-and-health).

Zha, Y., J. Gao, and S. Ni. 2003. "Use of Normalized Difference Built-up Index in Automatically Mapping Urban Areas from TM Imagery." *International Journal of Remote Sensing* 24 (3): 583–94. <https://doi.org/10.1080/01431160304987>.

Zhao, Hongbo, Zhibin Ren, and Juntao Tan. 2018. "The Spatial Patterns of Land Surface Temperature and Its Impact Factors: Spatial Non-Stationarity and Scale Effects Based on a Geographically-Weighted Regression Model." *Sustainability* 10 (7): 2242. <https://doi.org/10.3390/su10072242>.

Zhou, Manguo, Yanguo Huang, and Guilan Li. 2021. "Changes in the Concentration of Air Pollutants before and after the COVID-19 Blockade Period and Their Correlation with Vegetation Coverage." *Environmental Science and Pollution Research* 28 (18): 23405–19. <https://doi.org/10.1007/s11356-020-12164-2>.